J Mar Sci Technol (2004) 9:51–62
DOI 10.1007/s00773-003-0173-3

Journal of
Marine Science
and Technology

Original articles

Hydrodynamic optimization of ship hull forms in shallow water

Goutam Kumar Saha[1], Kazuo Suzuki[2], and Hisashi Kai[2]

[1]Department of Ocean and Space Engineering, Graduate School of Engineering, Yokohama National University, 79-5 Tokiwadai, Hodogaya-ku, Yokohama 240-8501, Japan
[2]Department of Ocean and Space Engineering, Faculty of Engineering, Yokohama National University, Yokohama, Japan

Abstract A computational method for improving hull form in shallow water with respect to wave resistance is presented. The method involves coupling ideas from two distinct research fields: numerical ship hydrodynamics and nonlinear programming techniques. The wave resistance is estimated by means of Morino's panel method, which is extended to free surface flow and considers the influence of finite depth on the wave resistance of ships. This is linked to the optimization procedure of the sequential quadratic programming (SQP) technique, and an optimum hull form can be obtained through a series of iterations giving some design constraints. Sinkage is an important factor in shallow water, and this method considers sinkage as a hydrodynamic design constraint. The optimization procedure developed is demonstrated by selecting a Wigley ($C_B = 0.444$) hull and the Series 60 ($C_B = 0.60$) hull, and new hull forms are obtained at Froude number 0.316. The Froude number specified corresponds to a lower than critical speed since most of the ships operating in shallow water move below their critical speed. The numerical results of the optimization procedure indicate that the optimized hull forms yields a reduction in wave resistance.

Key words Wave-making resistance · Shallow water · SQP · Sinkage

Introduction

The term "shallow water" is used to describe a body of water in which the boundaries are close to the ship only in the vertical direction. When the water becomes shallow, the resistance of a ship moving through it will become greater. The three-dimensional motion of the water will approach a two-dimensional character. The pressure set up by the ship's motion will be greater, and this extra pressure in shallow water causes larger waves than those in deep water. In shallow water, the lengths of waves accompanying the ship at a given speed are greater than those for the same speed in deep water. Furthermore, the change in stream velocities past the surface of the ship when in shallow water will slightly increase the resistance. It is important to know what happens when a hull form optimized for deep water operates in shallow water.

In shallow water, there is a phenomenon commonly referred to as squat that increases the draft of a ship while it is steaming. Squat is also present in deep water. Sinkage and trim, or squat, is important in very shallow water because of its practical consequences for underkeel clearance. In shallow water, it is common for a vessel to reach a state of operation known as the critical speed where, instead of a combination of diverging and transverse waves as seen in deep water, a new wave pattern is created which moves in the forward direction with the ship. This wave pattern is typically large, takes much energy to create, and can lead to severe environmental problems near the shore. At speeds greater or less than the critical speed, the steepness of the waves created and the resulting resistance are greatly reduced. Therefore, it is necessary to estimate the speed range through shallow-water areas and the wave-making resistance of the primary hull form design. Bangladesh, for example, is a riverine country. Some major rivers flow through the country and finally discharge into the Bay of Bengal, which surrounds the southern boundary. River craft, both large and small, play a very important role in the transportation of goods and passengers through the country. There is no doubt that the rivers and the Bay of Bengal are very significant in relation to the country's economic development. A striking feature of many rivers in Bangladesh is the vast shallow water areas, which necessitate strict draft requirements for ships.

Address correspondence to: G.K. Saha
(gsaha@mhl.shp.ynu.ac.jp)
Received: August 22, 2003 / Accepted: December 16, 2003

In order to solve a hydrodynamic problem like ship hull form optimization, the following elements are necessary: an evaluation method for an objective function related to hydrodynamic performance, a numerical optimization technique for the objective function, and a numerical shape deformation method for the ship hull form in the optimization process.

In recent years, computational fluid dynamics (CFD) methods have been introduced into the design process to simulate the flow field around the hull. CFD analysis is used as a replacement for tank testing. An interesting possibility is to combine a CFD method and a numerical method with a program for hull form variation. This procedure can be used to find a hull that is optimized with respect to properties computed by the CFD method, such as resistance, wave-height, sinkage, trim, etc. One or more geometrical constraints, e.g., displacement, and the main particulars and hydrodynamic constraints of the ship's hull such as sinkage, trim, etc., must be introduced to limit the modifications of the hull. A number of investigators have tried to employ optimization techniques in order to minimize some user-defined objective function in deep water, e.g., Hino,[1] Hino et al.,[2] Peri et al.,[3] and Tahara and Himeno.[4]

The effect upon resistance due to the changes in flow in shallow water has attracted the interest of scientists for many years. Havelock[5] studied the effects of shallow water on the wave resistance and wave pattern for a point-pressure impulse traveling over a free surface. Kinoshita and Inui[6] extended Havelock's theory to satisfy the bottoms boundary conditions more exactly. Kirch[7] used linearized wave theory to calculate the wave-making resistance for a simplified hull form in different water depths and channel widths. Muller[8] carried out extensive experiments and theoretical calculations based on linearized wave theory to investigate the effect of shallow water on wave-making resistance. Yasukawa[9] developed a first-order panel method based on Dawson's approach for the linear free-surface condition, and the shallow-water effect was found by replacing the bottom surface with rankine sources. Tarafder et al.[10,11] used Morino's panel method[12] to examine the influence of finite depth on the wave resistance of ships.

This article considers a hydrodynamic optimization problem for a ship hull in shallow water. In order to deal with it, a panel method applied to a free surface (PAFS) is used as the evaluation method for an objective function defined as wave-making resistance, and a nonlinear numerical sequential quadratic programming algorithm (SQP) is used as the numerical optimization technique of the objective function. PAFS is an extension form of Morino's panel[12] method to analyze the free-surface flow based on a Kelvin-type free-surface condition. A body shape is defined by the design variables, and the combination of design variable values which gives the hydrodynamic extremities of the body, such as minimum wave resistance under certain geometric and hydrodynamic constraints, is sought. If the sinkage is large, under-keel clearance will be low for a particular depth of water and may cause the ship to scrape the bottom. This circumstance should be borne in mind in the design process in order to ensure the safe operation of ships with a restricted draft. Therefore, sinkage is an important factor in shallow water, and this method considers it as an important hydrodynamic design constraint. The critical speed is related to the Froude number of the depth. The Froude number of the critical depth is 1.0. The optimization is carried out at a Froude number lower than the Froude number of the critical depth since most ships operate below the critical speed for any particular depth of water. In this optimization problem, the wave resistance has been selected as a single objective function.

Outline of the formulation

Let us consider two coordinate systems in which x'–y'–z' is fixed with respect to the ship, and x–y–z is a steady moving frame of reference with forward speed U in the positive x-direction. The origin of the coordinate system x–y–z (shown in Fig. 1) is located in calm water. The z-axis is upward and the y-axis extends to starboard. The depth of water is h. The fluid is assumed to be inviscid and incompressible, and its motion is irrotational such that the velocity potential of the fluid Φ can be defined as

$$\Phi = \mathrm{U}x + \sum_{n=1}^{\infty} \varepsilon^n \phi_n + \mu\left(s\varphi_s + t\varphi_t\right) \tag{1}$$

where ε and μ are two small parameters, ϕ is the steady perturbation potential in the absence of sinkage and trim, φ_s is the steady potential due to unit sinkage, φ_t is the steady potential due to unit trim, s is the sinkage (positive upward), and t is the trim angle (trim by the stern is positive). The potential Φ satisfies the Laplace equation

$$\nabla^2 \Phi = 0 \tag{2}$$

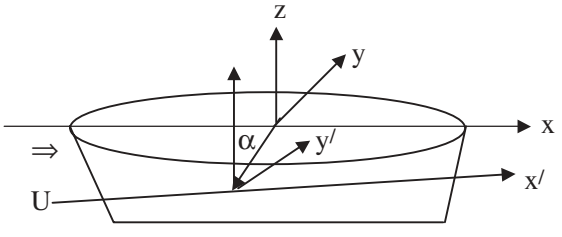

Fig. 1. Definition sketch of the coordinate system

in the fluid domain V. The fluid domain V is bounded by the hull surface S_H, the free surface S_F, the sea bottom surface S_B, and the surface at infinity S_∞.

A boundary value problem can be constructed by specifying the boundary conditions on the boundary, as described below.

1. Hull surface (S_B) boundary condition:

$$\left.\begin{aligned} &\varepsilon: \quad \nabla\phi_1 \cdot \mathbf{n} = -Un_x \\ &\varepsilon^2: \quad \nabla\phi_2 \cdot \mathbf{n} = 0 \end{aligned}\right\} \tag{3}$$

with respect to sinkage and trim

$$\left.\begin{aligned} &\varepsilon^2: \quad \nabla\varphi_s \cdot \mathbf{n} = m_3 \\ &\varepsilon^2: \quad \nabla\varphi_t \cdot \mathbf{n} = m_5 \end{aligned}\right\} \tag{4}$$

with

$$\mathbf{i}\cdot.m_1 + \mathbf{j}\cdot m_2 + \mathbf{k}\cdot.m_3 = -(\mathbf{n}\cdot\nabla)\mathbf{W}$$
$$\mathbf{i}\cdot.m_4 + \mathbf{j}\cdot m_5 + \mathbf{k}\cdot.m_6 = -(\mathbf{n}\cdot\nabla)(x\times\mathbf{W})$$
$$\mathbf{W} = \mathbf{U} + \nabla\phi_1$$

where

$$\mathbf{n} = \mathbf{i}\cdot n_x + \mathbf{j}\cdot n_y + \mathbf{k}\cdot n_z$$

is the unit normal vector and is positive into the fluid.

2. Free surface boundary condition:

$$\left.\begin{aligned} &\varepsilon: \quad \phi_{1xx} + K_0\phi_{1z} = 0 \\ &\varepsilon^2: \quad \phi_{2xx} + K_0\phi_{2z} = f(\phi_1) \end{aligned}\right\} \quad \text{on } z = 0 \tag{5}$$

$$f(\phi_1) = -\frac{1}{U}\frac{\partial}{\partial x}\left(\phi_{1x}^2 + \phi_{1y}^2 + \phi_{1z}^2\right) - \zeta_1\frac{\partial}{\partial z}\left(\phi_{1xx} + K_0\phi_{1z}\right)$$

with respect to sinkage and trim

$$\left.\begin{aligned} &\varepsilon^2: \ \phi_{sxx} + K_0\phi_{sz} = 0 \\ &\varepsilon^2: \ \phi_{txx} + K_0\phi_{tz} = 0 \end{aligned}\right\} \quad \text{on } z = 0 \tag{6}$$

where $K_0 = g/U^2$ is the wave number.

3. Bottom boundary condition and radiation condition:

$$\left.\begin{aligned} &\varepsilon: \ \nabla\phi_1\cdot n = 0 \qquad \varepsilon^2: \nabla\phi_2\cdot n = 0 \\ &\varepsilon^2: \nabla\phi_s\cdot n = 0 \qquad \varepsilon^2: \nabla\phi_t\cdot n = 0 \end{aligned}\right\} \quad \text{on } z = -h \tag{7}$$

Finally, it is necessary to impose the conditions that there are no waves far upstream of the ship, and the waves are always traveling downstream.

Calculation of the hydrodynamic forces acting on a ship

The fluid pressure acting on the instantaneous wetted surface of ship hull S_H during oscillatory motions of the ship can be written according to Bernoulli's equation as

$$p - p_\infty = \frac{1}{2}\rho\left(U^2 - \nabla\Phi.\nabla\Phi\right) - \rho gz$$

The pressure at any point on the wetted surface S_H can be expressed in terms of the pressure at the corresponding point of the surface S_0 at mean water level.

$$\left[p - p_\infty\right]_{S_H} = \left[1 + (\alpha.\nabla) + \frac{1}{2}(\alpha.\nabla)^2 + \ldots\right]\left(p - p_\infty\right)_{S_0}$$

where α is the oscillatory displacement of the ship, which will be obtained from the transformation of the coordinate system as (tz', 0, s-tx'). It is assumed that the displacement α is so small that the second-order terms may be neglected, and then the linearized form of the pressure on the wetted surface S_H becomes

$$p - p_\infty = \frac{1}{2}\rho\left(U^2 - \nabla\Phi.\nabla\Phi\right) + \frac{1}{2}\rho(\alpha.\nabla)\left(U^2 - \nabla\Phi.\nabla\Phi\right) - \rho gz + 0(\alpha)$$

The hydrodynamic forces (k = 1,2,3 indicate surge, sway, and heave, respectively) and moments (k = 4,5,6 indicate rolling, pitching, and yawing, respectively) in the kth direction can be represented by

$$F_k = -\int\left(p - p_\infty\right).n_k\,\mathrm{d}S \approx F_k^0 + sF_k^S + tF_k^t \tag{8}$$

Sinkage and trim calculation

The sinkage and trim of a ship moving in shallow water can be computed by equating the vertical force and pitch moment to the hydrostatic restoring force and moment. The following equations are then obtained from the static equilibrium of forces.

$$F_3 = s\rho g\int_{-L/2}^{L/2} f_w(x)\mathrm{d}x - t\rho g\int_{-L/2}^{L/2} f_w(x)x\mathrm{d}x \tag{9}$$

$$F_5 = -s\rho g\int_{L/2}^{L/2} f_w(x)x\mathrm{d}x + t\rho g\int_{-L/2}^{L/2} f_w(x)x^2\mathrm{d}x \tag{10}$$

where $f_w(x)$ is the width of the water plane area at the still water level, and L denotes the length of the ship. By combining Eqs. 8, 9, and 10, the values of s and t can be obtained.

Wave-resistance calculation

The wave resistance can be calculated by integrating the pressure over the hull surface up to the mean water level, and including the waterline, which is calculated by

$$R_w = F_1^0 + sF_1^s + tF_1^t - \frac{1}{2}\rho g \oint_{w1} \zeta^2 n_x \mathrm{d}\ell - \oint_{w1} F_1^0(s - tx) n_x \mathrm{d}\ell \tag{11}$$

The first-term integral on the right-hand side of Eq. 11 represents the correction of the difference between the real and still water levels, and the second-term integral on the right-hand side represents the correction between the real and still water due to sinkage and trim.

The wave-making resistance coefficient C_w is obtained by

$$C_w = \frac{R_w}{\frac{1}{2}\rho S U^2} \tag{12}$$

where S is the hull surface wetted area and ρ is the fluid density.

The boundary integral equation which satisfies the boundary value problem above can be written as

$$\begin{aligned} \pi E\phi(p) = &\sum_{i=1}^{N_H} \int_{S_H} \phi(q) \frac{\partial G}{\partial n_q} \mathrm{d}S - \sum_{i=1}^{N_H} \int_{S_H} \frac{\partial \phi(q)}{\partial n_q} G \mathrm{d}S \\ &+ \sum_{i=1}^{N_B} \int_{S_B} \phi(q) \frac{\partial G}{\partial n_q} \mathrm{d}S - \sum_{i=1}^{N_F} \int_{S_F} \frac{\partial \phi(q)}{\partial n_q} G \mathrm{d}S \end{aligned} \tag{13}$$

where

$$E = \frac{1}{2} \text{ on } S_H,\ S_B$$
$$= \frac{1}{4} \text{ on } S_F$$
$$G = \frac{1}{R} + \frac{1}{R'}$$
$$R = \sqrt{(x - x')^2 + (y - y')^2 + (z - z')^2}$$

In Eq. 12, $P(x,y,z)$ is a filed point, $Q(x,y,z)$ is a control point, G is the green function, and R' is the image of R. The solution is obtained by replacing the hull, free surface, and sea bottom with a distribution of sources and dipoles. The surfaces are discretized into flat quadrilateral elements, and the influence coefficients are calculated using Morino's panel[12] method.

Details of the above mathematical calculations for shallow water analysis are given by Tarafder et al.[10,11] The wave profiles measured and the wave-making resistance of an Inuid S-201 hull were used to validate the computer program developed. The theoretical values obtained by the present PAFS show good agreement with experimental values for the Inuid S-201 hull found by Muller.[8]

Nonlinear optimization technique

The sequential quadratic programming (SQP) method is a general method for solving nonlinear optimization problems with constraints. Let the optimization problem be written as

$$\begin{aligned} &\text{Minimize} && F[X] \\ &\text{subject to} && h_j[X] = 0, \quad j = 1, M_e \\ &&& g_j[X] \le 0, \quad j = M_e + 1, M_i \end{aligned}$$

where F is an objective function, and h_j and g_j are equality and inequality constraints, respectively. When the current design point is $X^{(k)}$, the next design point $X^{(k+1)}$ is determined as follows. First, the following quadratic programming problem is solved to obtain the modification of **d**.

$$\text{Minimize} \quad \nabla F\left[X^{(k)}\right]^T \cdot \mathbf{d} + \frac{1}{2}\mathbf{d}^T \mathbf{H}^{(k)} \cdot \mathbf{d}$$

subject to

$$h_j\left[X^{(k)}\right] + \nabla h_j\left[X^{(k)}\right]^T \cdot \mathbf{d} = 0, \quad j = 1, M_e$$
$$g_j\left[X^{(k)}\right] + \nabla g_j\left[X^{(k)}\right]^T \cdot \mathbf{d} \le 0, \quad j = 1 + M_e, M_i$$

Here, the objective function F is approximated as the quadratic function of $X^{(k)}$, and the constraints are approximated as the linear functions of $X^{(k)}$. H is an approximation to the Hessian matrix of the Lagrangian

$$H = \nabla^2 F + \sum_{j=1}^{M_e} u_j \nabla^2 h_j + \sum_{j=1}^{M_i} v_j \nabla^2 g_j$$

where $u = (u_1,u_2,u_3, \ldots)^T$ and $v = (v_1,v_2,v_3, \ldots)^T$ are the Lagrangian multipliers for equality and inequality constraints, respectively.

The next design point $X^{(k+1)}$ is obtained by the line search along the vector **d**. The step-size δ is determined in such a way that the penalty function with r, being a penalty parameter

$$F[X] + r\left\langle \sum_{j=1}^{M_e} |h_j[X]| + \sum_{j=M_e+1}^{M_i} |\min(0, g_j[X])| \right\rangle$$

becomes smaller than a set value. Finally, the next design point is computed by

$$X^{(k+1)} = X^{(k)} + \delta^{(k)} d^{(k)}$$

The Hessian matrix is updated using the Broyden, Fletcher, Goldfarb, and Shanon (BFGS) method, as follows:

$$H^{(k+1)} = H^k + \frac{\gamma\gamma^T}{q^T s} - \frac{H^{(k)} s s^T H^{(k)}}{s^T H^{(k)} s}$$

Where

$$s = X^{(k+1)} - X^{(k)}, \qquad q = \nabla_x L^{(k+1)} - \nabla_x L^{(k)}$$

$$\nabla_x L = \nabla F + \sum_{j=1}^{M_e} u_j \nabla h_j + \sum_{j=1}^{M_i} v_j \nabla g_j$$

$$\gamma = \theta q + (1-\theta) H^{(K)} s$$

$$\theta = \begin{cases} 1.0 & \text{if } q^{\mathrm{T}} s \geq 0.2 s^{\mathrm{T}} H^{(k)} s \\ \dfrac{0.8 s^{\mathrm{T}} H^{(k)} s}{s^{\mathrm{T}} H^{(k)} s - q^{\mathrm{T}} s} & \text{if } q^{\mathrm{T}} s < 0.2 s^{\mathrm{T}} H^{(k)} s \end{cases}$$

Hull form modification function

The selection of a hull form modification function is important in the optimization process because the function must have sufficient expressiveness for the desired hull modification. Also, as the number of design parameters of the function increases, the computational time required in the optimization procedure increases significantly.

The modification quantity from the original form $y(x,z)$ is assumed to be

$$y(x,z) = y_0(x,z) w(x,z) \tag{14}$$

where $y_0(x,z)$ is the original hull surface defined in longitudinal and vertical coordinates (x,z). In this form, depth-wise modification is not considered. $W(x,z)$ is a weight function to provide a transverse-directional expansion and reduction ratio, which for an aft body is given by

$$w(x,z) = 1 - \sum_{m=1} \sum_{n=1} \alpha_{mm} \sin\left\{ \pi \left(\frac{x - x_0}{x_{\min} - x_0} \right)^{m+2} \right\} \times \sin\left\{ \pi \left(\frac{\beta - z}{\beta + T} \right)^{n+2} \right\}, \qquad -L/2 \leq x \leq 0 \tag{15}$$

and by

$$w(x,z) = 1 - \sum_{m=1} \sum_{n=1} \alpha_{mm} \sin\left\{ \pi \left(\frac{x - x_0}{x_{\max} - x_0} \right)^{m+2} \right\} \times \sin\left\{ \pi \left(\frac{\beta - z}{\beta + T} \right)^{n+2} \right\}, \qquad 0 \leq x \leq L/2 \tag{16}$$

for a fore body. x_0, $x_{\max}$, $x_{\min}$, T are parameters for characterizing the hull form modification (hull form parameters), and α_{mn}, β are taken as the design variables in the optimization procedure. Stem and stern profiles cannot be modified in hull form improvement when using this formula.

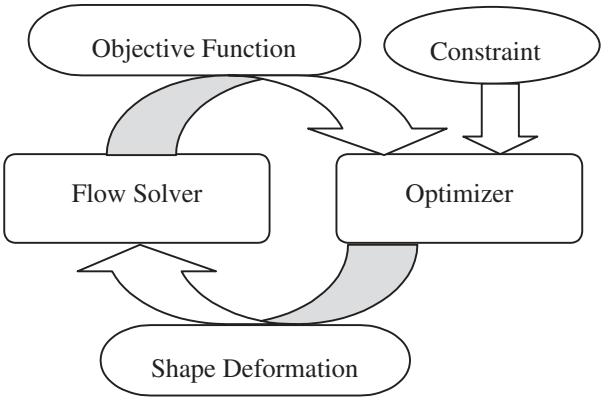

Fig. 2. Iterative process for the shape

Optimization method for a hull form

The numerical optimization can be carried out by systematic iterative evaluations of the objective function, as in the concept in Fig. 2. In general engineering optimization problems, the objective functions are nonlinear with respect to the design variables, and complex design constraints are imposed. To solve such optimization problems a nonlinear programming (NLP) technique should be employed.

In the present study, SQP[13,14] is selected as one of the NLP techniques to minimize the objective function under design constraints.

The method of finding a form with a lower resistance is now described. Optimization is carried out so as to yield a hull form with lower resistance. The objective function is the wave resistance coefficient, that may be calculated using Eq. 12.

The ship's hull was subjected to the following geometric and hydrodynamic constraints.

1. The displacement must be greater than the original value.
2. The position of longitudinal center of buoyancy (LCB) should not be less than 2% of L_{PP} from its original position and not greater than 2% of L_{PP} from its original position.
3. The water plane area must be greater than the original value.
4. The sinkage must be less than the original value.

In the optimization procedure, the variables to be altered are the y coordinates of the ship's hull. The body shape is modified by Eqs. 14–16.

Numerical optimization was first carried out on the mathematical Wigley hull ($C_{\mathrm{B}} = 0.444$) and then on the Series 60 hull ($C_{\mathrm{B}} = 0.60$). The forms were optimized at the single Froude number ($\mathrm{Fn} = U/\sqrt{gL}$) of 0.316, which corresponds to the lower critical-depth Froude number ($\mathrm{Fn}_h = U/\sqrt{gh}$) for a particular depth of water for both

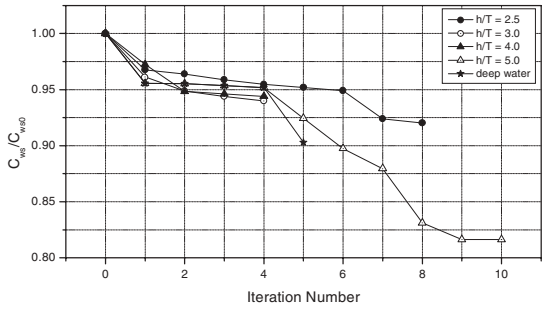

Fig. 3. Convergence history of the wave resistance of the Wigley hull

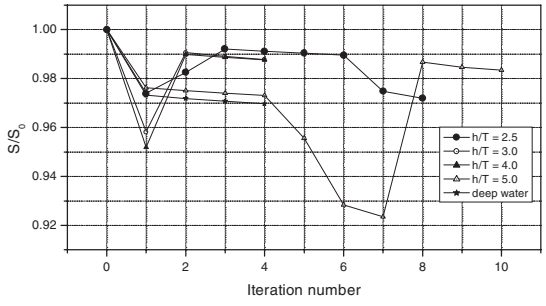

Fig. 4. Convergence history of the sinkage of the Wigley hull for different water depths

models. The Froude number was based on the length between perpendiculars ($L_{pp} = L$). The geometric and hydrodynamic design constraints which have been imposed for both the Wigley model and the Series 60 ($C_B = 0.6$) are described above. The number of panels on the hull, the free surface, and the sea bottom were taken as 40×10, 70×15, and 40×10, respectively, for both models. The total number of design variables was 10.

Results and discussion

Optimization of the Wigley hull

The first application is for the optimization of the Wigley hull ($C_B = 0.444$) form with respect to the minimum wave-making resistance. This hull form is optimized at water depths $h/T = 2.5$, 3.0, 4.0, 5.0, and deep water in order to compare the hydrodynamic behavior in shallow and deep water.

The convergence histories of the wave-making resistance and sinkage of the Wigley hull by the SQP process are shown in Figs. 3 and 4, respectively. Optimization at $h/T = 2.5$, 3.0, 4.0, 5.0, and deep water yielded converged solutions at 8, 4, 4, 10, and 5 optimization cycles, respectively. The wave resistance decreased by approximately 8% at $h/T = 2.5$, by approximately 6% at $h/T = 3.0$ and 4.0, by approximately 17% at $h/T = 5.0$, and by approximately 10% at $h/T = \infty$. Application of the optimization procedure produced optimal hulls with original bodyplans as shown in Figs. 5–9 at depths of $h/T = 2.5$, 3.0, 4.0, 5.0, and deep water, respectively. The resulting forms are entirely dictated by the hydrodynamic behavior associated with the changes in hull shape, and the optimized hull form has scarcely deviated from the original hull. Figure 10 shows comparisons of the sectional areas of the original and optimized hulls at different water depths. The sectional area has decreased near the amidships region and increased towards the fore part (FP) and aft part (AP). The comparisons between the original and calculated wave profiles along the hull

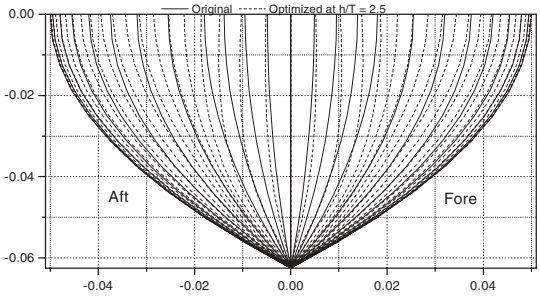

Fig. 5. Comparison of body plans of the Wigley hull at $h/T = 2.5$

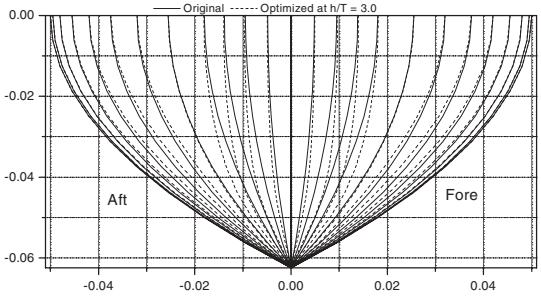

Fig. 6. Comparison of body plans of the Wigley hull at $h/T = 3.0$

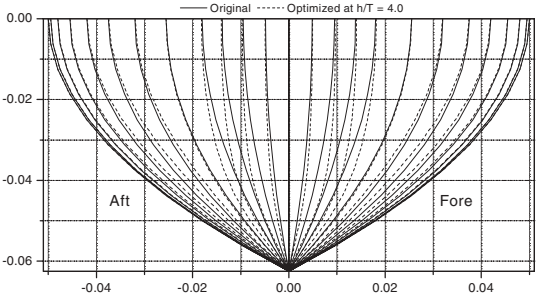

Fig. 7. Comparison of body plans of the Wigley hull at $h/T = 4.0$

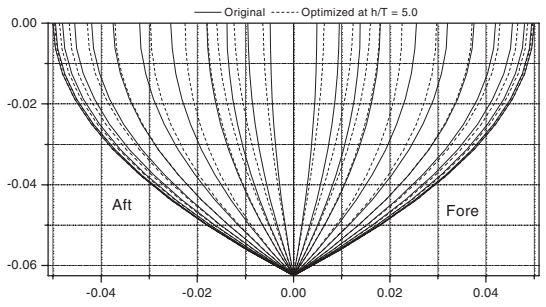

Fig. 8. Comparison of body plans of the Wigley hull at $h/T = 5.0$

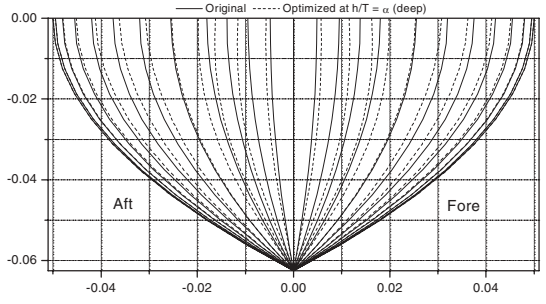

Fig. 9. Comparison of body plans of the Wigley hull in deep water

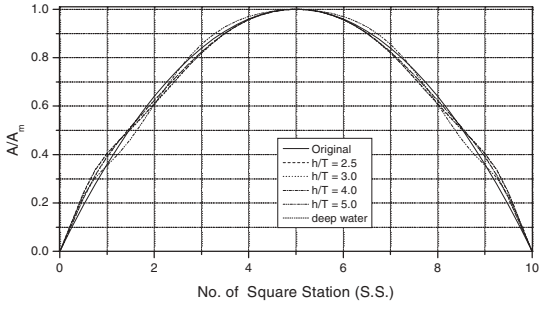

Fig. 10. Comparison of the sectional area curve of the Wigley hull for different water depths

are shown in Figs. 11–15 at $h/T = 2.5$, 3.0, 4.0, 5.0, and deep water, respectively. The wave profiles were taken from the free-surface elevation at panels adjacent to the ship hull surface. The optimized hull generates a slightly greater wave height at the bow than the original hull. This is due to the increased steepness of the waves created at the bow. The amplitude of the stern waves is lower than with the original hull, and this is due to a reduction of the transverse wave system. Figures 16–20 show the contours of the nondimensional wave pattern calculated for optimized hulls (upper) and the corresponding wave patterns for the original hull (lower) at water depths $h/T = 2.5$, 3.0, 4.0, 5.0, and deep water,

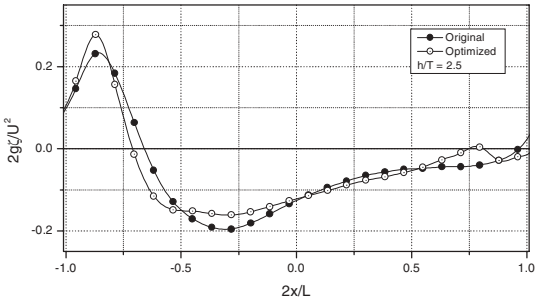

Fig. 11. Comparison of the wave profiles along the Wigley hull at $h/T = 2.5$

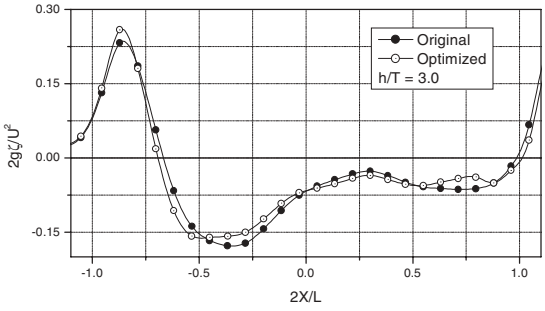

Fig. 12. Comparison of the wave profiles along the Wigley hull at $h/T = 3.0$

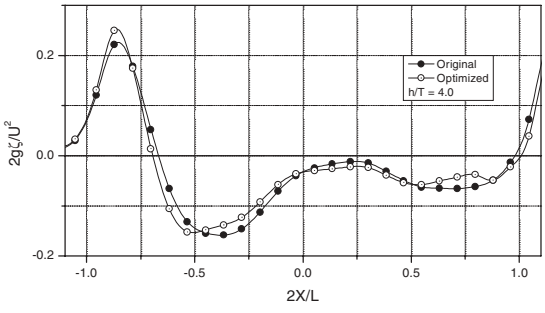

Fig. 13. Comparison of the wave profiles along the Wigley hull at $h/T = 4.0$

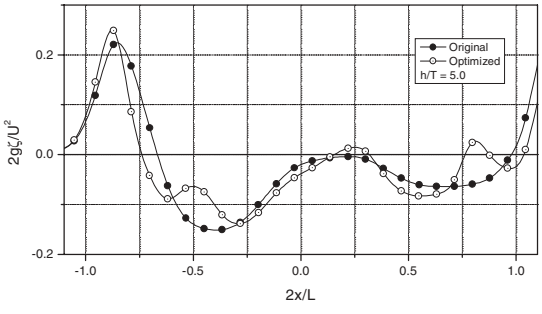

Fig. 14. Comparison of the wave profiles along the Wigley hull at $h/T = 5.0$

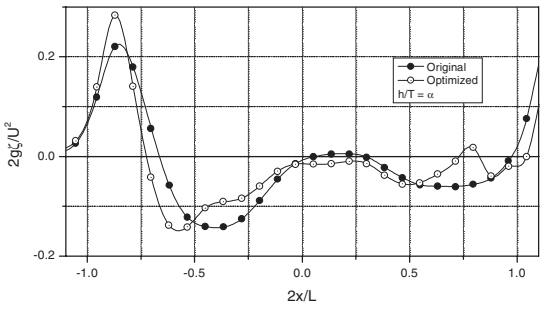

Fig. 15. Comparison of the wave profiles along the Wigley hull in deep water

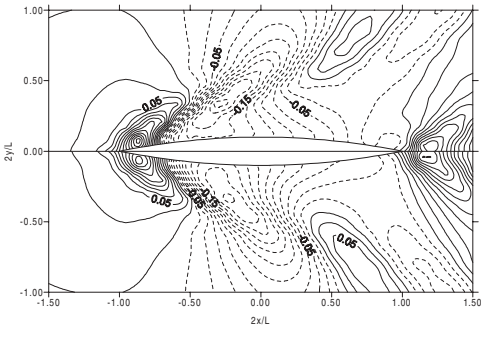

Fig. 16. Wave patterns ($2g\zeta/U^2$) at water depth $h/T = 2.5$

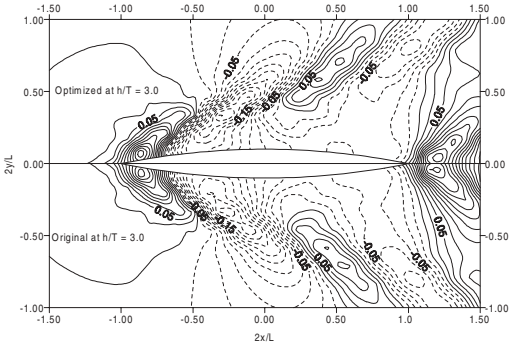

Fig. 17. Wave patterns ($2g\zeta/U^2$) at water depth $h/T = 3.0$

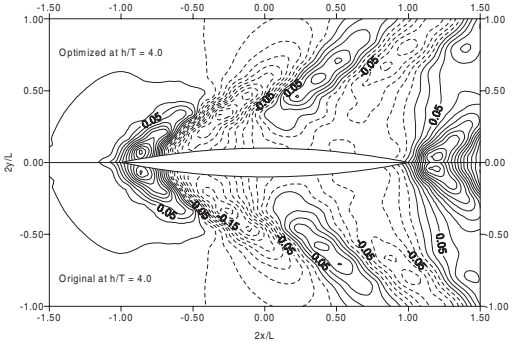

Fig. 18. Wave patterns ($2g\zeta/U^2$) at water depth $h/T = 4.0$

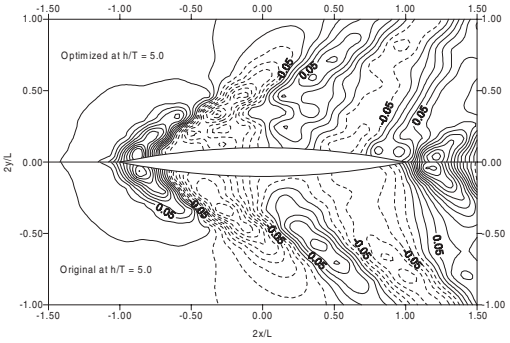

Fig. 19. Wave patterns ($2g\zeta/U^2$) at water depth $h/T = 5.0$

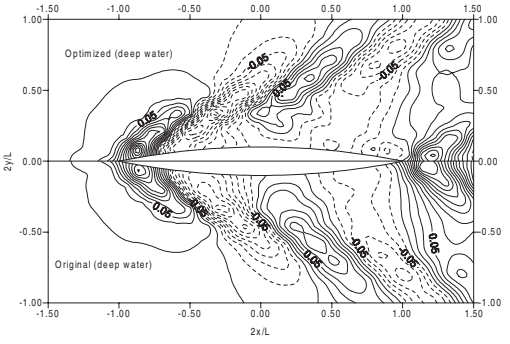

Fig. 20. Wave patterns ($2g\zeta/U^2$) at deep water

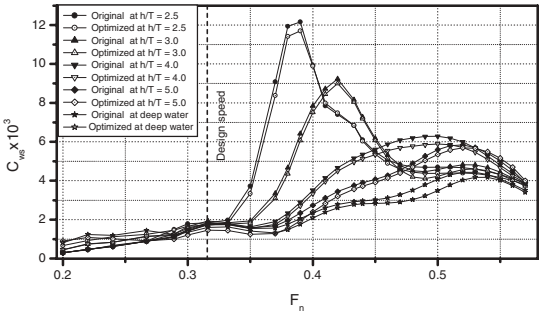

Fig. 21. Comparison of wave resistance for different water depths at Fn = 0.316

respectively. The differences in the wave fields generated by optimized hulls and the original hull are clear. Finally, Fig. 21 shows comparisons of the wave-resistance coefficient for the optimized and original hulls. It can be seen that a reduction in the wave-resistance coefficient has been achieved. Although the wave height at the bow is slightly higher than the original one, and the hull form has been optimized for a single speed (Fn = 0.316), which corresponds to a lower critical speed for different depths of water, the optimized forms have less wave resistance over a wide range of design speeds.

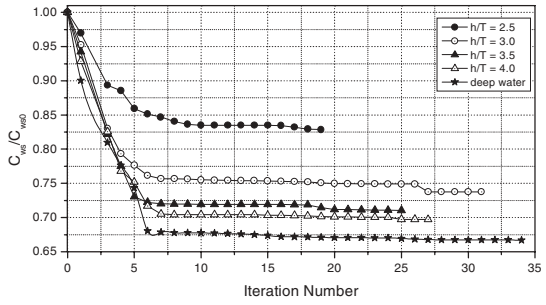

Fig. 22. Convergence history of wave resistance for the Series 60 ($C_B = 0.6$) hull

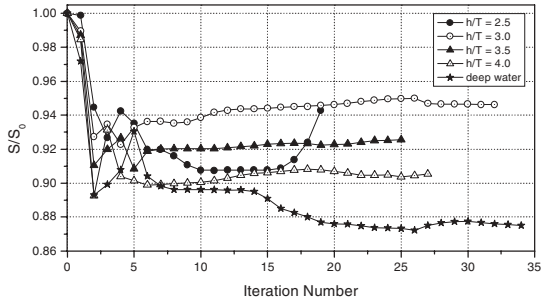

Fig. 23. Convergence history of sinkage for the Series 60 ($C_B = 0.6$) hull

Optimization of Series 60 ($C_B = 0.6$)

For the second example, a well-known hull shape, the Series 60 ($C_B = 0.6$), was selected as the initial body shape. This is a standard ship hull which has been used extensively as a design reference. This hull is optimized at water depths $h/T = 2.5$, 3.0, 3.5, 4.0, and deep water in order to verify its hydrodynamic behavior in shallow and deep water. Figures 22 and 23 show the convergence history of wave resistance and sinkage for the Series 60 hull. Optimization at $h/T = 2.5$, 3.0, 3.5, 4.0, and deep water yielded converged solutions at 19, 31, 25, 27, and 35 optimization cycles, respectively. The wave resistance decreased by about 17% at water depth $h/T = 2.5$, by about 27% at water depth $h/T = 3.0$, by about 29% at water depth $h/T = 3.5$, by about 30% at water depth $h/T = 4.0$, and by about 33% at water depth $h/T = \infty$. Application of the optimization procedure produced optimal hulls with the original body plans shown in Figs. 24–28 at water depths $h/T = 2.5$, 3.0, 3.5, 4.0, and deep water, respectively. The frame lines of the fore part become U-shaped for the modified hull, and this effectively makes the water plane narrower and moves the volume from the upper to the lower region. The frame lines of the aft part of the optimized hull change from U-shaped to V-shaped, which means that the water plane is wider than the original hull to compensate for displacement loss in the bow part and the volume shift from the lower to the upper region. Figure 29 shows the difference in sectional area between the original and optimized hulls at different depths of water. The sectional area has decreased near the amidships region and increased towards the FP and AP. Comparisons between the calculated wave profiles along the hull are shown in Fig. 30–34 at $h/T = 2.5$, 3.0, 3.5, 4.0, and deep water, respectively. The wave profiles were taken from the free-

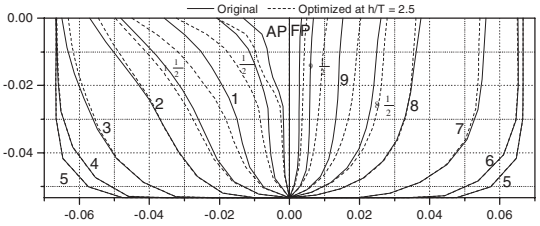

Fig. 24. Comparison of body plans for the Series 60 ($C_B = 0.6$) at $h/T = 2.5$

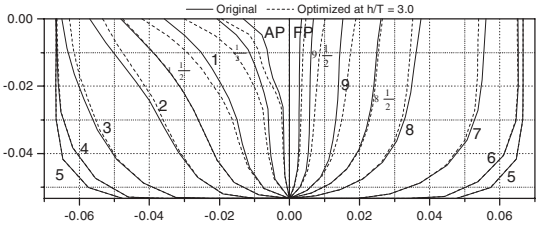

Fig. 25. Comparison of body plans for the Series 60 ($C_B = 0.6$) at $h/T = 3.0$

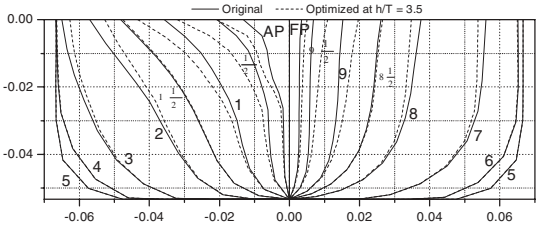

Fig. 26. Comparison of body plans for the Series 60 ($C_B = 0.6$) at $h/T = 3.5$

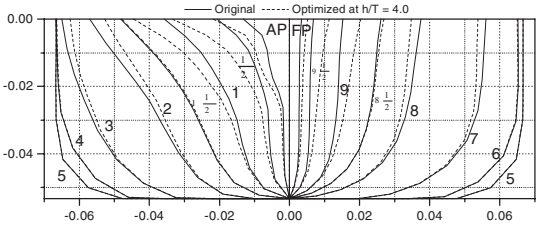

Fig. 27. Comparison of body plans for the Series 60 ($C_B = 0.6$) at $h/T = 4.0$

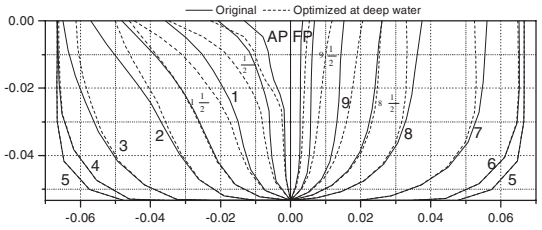

Fig. 28. Comparison of body plans for the Series 60 ($C_B = 0.6$) in deep water

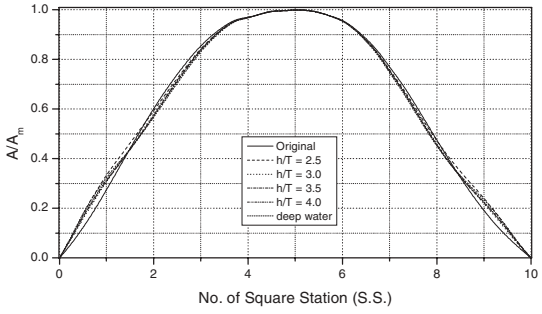

Fig. 29. Comparison of the sectional area curves for different water depths

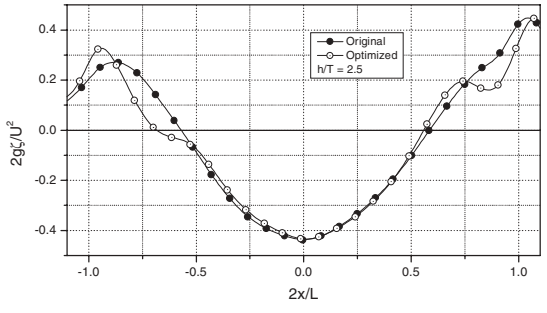

Fig. 30. Comparison of wave profiles along the hull at h/T = 2.5

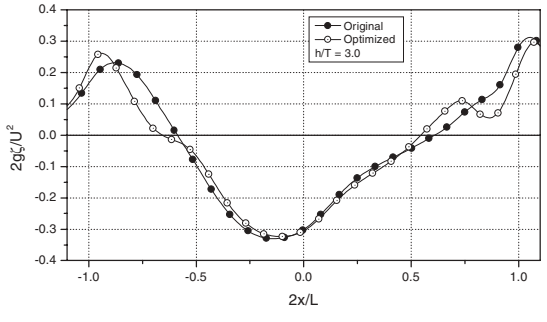

Fig. 31. Comparison of wave profiles along the hull at h/T = 3.0

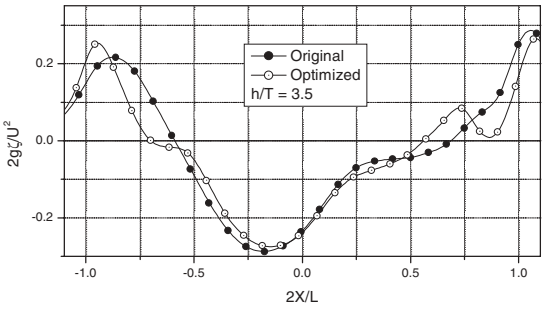

Fig. 32. Comparison of wave profiles along the hull at h/T = 3.5

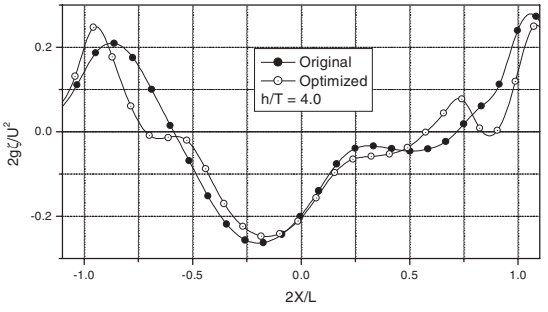

Fig. 33. Comparison of wave profiles along the hull at h/T = 4.0

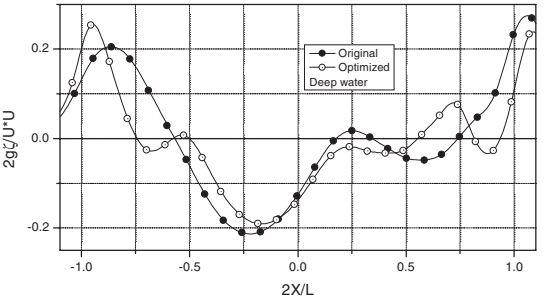

Fig. 34. Comparison of wave profiles along the hull in deep water

surface elevation at panels adjacent to the ship's surface. The optimized hull generates a slightly greater bow wave than the original hull. The increase in the steepness of the bow wave is one of the reasons. The amplitude of the stern waves is less than with the original hull, and this is due to the reduction of the transverse wave system. Figures 35–39 give the contours of the nondimensional wave pattern calculated for optimized hulls (upper) and the corresponding wave patterns for the original hull (lower) at h/T = 2.5, 3.0, 3.5, 4.0, and deep water, respectively. The difference in the wave fields generated by modified hulls and the original hull are clear. Lastly, Fig. 40 shows comparisons of the wave-resistance coefficient for the modified hull and

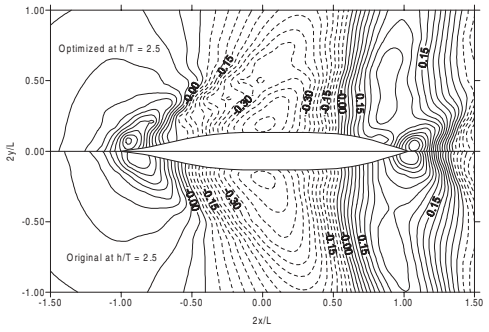

Fig. 35. Wave patterns ($2g\zeta/U^2$) at water depth $h/T = 2.5$

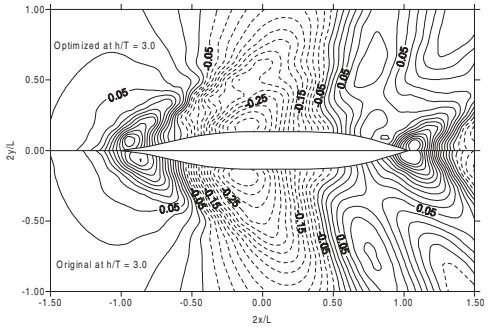

Fig. 36. Wave patterns ($2g\zeta/U^2$) at water depth $h/T = 3.0$

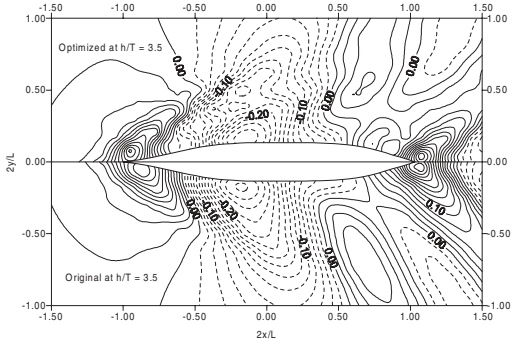

Fig. 37. Wave patterns ($2g\zeta/U^2$) at water depth $h/T = 3.5$

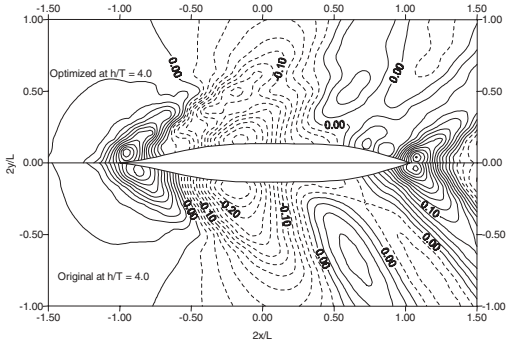

Fig. 38. Wave patterns ($2g\zeta/U^2$) at water depth $h/T = 4.0$

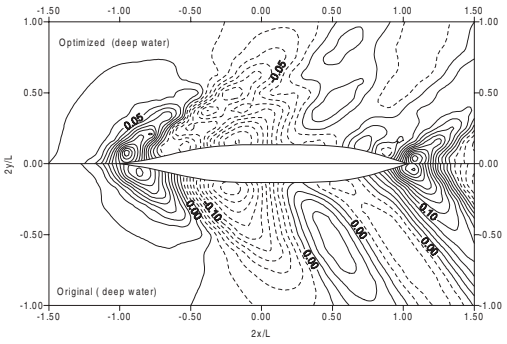

Fig. 39. Wave patterns ($2g\zeta/U^2$) in deep water

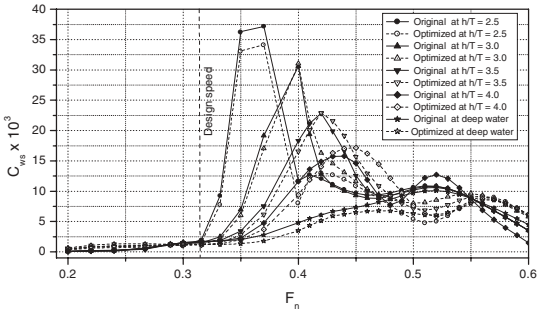

Fig. 40. Comparison of wave resistance for different water depths

the original Series 60 ($C_B = 0.6$). It can be seen that a reduction in the wave-resistance coefficient has been achieved. Although the height of the bow wave is greater than the original value, and the hull form has been optimized for a single speed (Fn = 0.316), which corresponds to a lower critical speed for different depths of water, the optimized forms have less wave resistance over a wide range of design speeds.

Conclusions

A numerical method has been proposed for hull-form optimization in shallow water with respect to wave resistance. By combining a numerical method for solving the three-dimensional potential flow around a ship moving at a constant speed in calm, shallow water with the SQP technique, an improved hull form with lower resistance can be generated through a series of iterations.

The system was applied to two optimization problems. The first was for a mathematical Wigley (C_B = 0.44) hull with minimum wave resistance in different water depths. The second was the minimization by wave resistance by the Series 60 ($C_B = 0.60$) hull as a standard model for the development of optimal ship hull forms.

The numerically obtained results were compared with the original values, and a reduction in wave resistance was achieved at all water depths. Sinkage was also reduced at all water depths. Comparisons of the results from the original and optimized (both Wigley and Series 60) hulls allowed identification of the salient differences in flow features which can be used in hull-form design. Since sinkage is of practical importance in shallow water, it was considered as a hydrodynamic constraint during the optimization. The Froude number 0.316 was selected because most ships in shallow water operate below their critical speed at any particular water depth, and sinkage is the dominant effect in the subcritical regime. In the selection of the hull-form modification function, only beam-wise modification was considered, and depth-wise modification was ignored. However, in shallow water depth-wise modification is important, so no significant difference was observed in the optimized hull forms in deep and shallow waters. In future, depth-wise modification will also be considered. In conclusion, the results presented here indicate that this method could be used in practical hull-form designs for ships operating in a shallow-water region.

The method presented here is only the beginning of the work done to develop a complete optimum hull-form design system. Not all the important factors for determining a ship's performance have been incorporated in this system. In particular, it is important in the design of ships that propulsion and sea-keeping are considered at an early design stage. Furthermore, a determination of the optimal principal particulars of the ship is also an integral part of the design process. Although the method presented has not yet been exploited and tested under sufficiently broad conditions or in a reasonable number of cases, the results indicate that the optimization procedure works, and that an optimum hull form can be obtained.

Acknowledgments. The first author is very grateful to the Ministry of Education, Culture, Sports, Science and Technology of Japan, whose doctoral course scholarship made the present research possible. The authors would also like to thank Emeritus Prof. M. Ikehata for valuable suggestions.

References

1. Hino T (1996) Fluid dynamic shape optimization using sensitivity analysis of Navier–Stokes solutions. J Kansai Soc Nav Archit Jpn (126):49–54
2. Hino T, Kodama Y, Hirata N (1998) Hydrodynamic shape optimization of ships hull forms using CFD. In: Proceedings of the 3rd Osaka Colloquium on Advanced CFD Applications to Ship Flow and Hull Form Design, Osaka, Japan, pp 533–541
3. Peri D, Rossetti M, Campana EF (2001) Design optimization of ship hulls via CFD technologies. J Ship Res 45:140–149
4. Tahara Y, Himeno Y (1998) An application of computational fluid dynamics to ship hull optimization problem. In: Proceedings of the 3rd Osaka Colloquium on Advanced CFD Applications to Ship Flow and Hull Form Design, Osaka, Japan, pp 515–531
5. Havelock TH (1922) The effect of shallow water on wave resistance. Proc R Soc London 100:499–505
6. Kinoshita M, Inui T (1953) Wavemaking resistance of submerged spheroid ellipsoid and ship in shallow sea. J Soc Nav Archit Jpn 75:119–135
7. Kirsch M (1966) Shallow water and channel effects on wave resistance. J Ship Res 10:164–181
8. Muller E (1985) Analysis of potential flow field and of ship resistance in water of finite depth. Int Shipbuilding Prog 32(376):266–277
9. Yasukawa T (1989) Calculation of free surface flow around a ship in shallow water by Rankine source method. In: 5th International Conference on Numerical Ship Hydrodynamics, Hiroshima, Japan, pp 643–653
10. Tarafder MD, Suzuki K, Kai H (2002) Wavemaking resistance of ships in shallow water based on second-order free surface condition with sinkage and trim effects. J Kansai Soc Nav Archit Jpn (237):9–17
11. Tarafder MD, Suzuki K, Kai H (2002) Free surface potential flow around multi-hulls in shallow water using a potential-based panel method. J Kansai Soc Nav Archit Jpn (238):29–38
12. Suciu EO, Morino L (1976) A nonlinear finite element analysis for wings in steady incompressible flows with wake roll-up. AIAA Paper No. 76-64, pp 1–10
13. ASNOP (1991) Research group: application systems for nonlinear optimization problems (in Japanese). Nikkan Kogyo Shimbun, Tokyo
14. Bhatti MA (2000) Practical optimization methods with mathematical applications. 1st edn. Springer, New York